© *Proc. Indian natn. Sci. Acad.*, **52**, A, No. 1, 1986, pp. 117–134
Printed in India.

LOW-DIMENSIONAL FERROMAGNETIC COMPOUNDS : RECENT DEVELOPMENTS*

P DAY

Oxford University, Inorganic Chemistry Laboratory, South Parks Road, Oxford OX1 3QR, England

(*Received 4 December 1985*)

After an introductory survey of the unusual physical properties associated with low-dimensional lattices recent developments in the study of low-dimensional inorganic compounds with near-neighbour ferromagnetic exchange interactions are reviewed with special reference to work on magnetic structures and phase transitions carried out by the Oxford group. The structural circumstance leading to ferromagnetism through superexchange are noted, and bulk magnetic and neutron scattering experiments on each category are surveyed. Canted and incommensurate magnetic structures are described. Studies of the mechanism of the transition to long range order are summarized.

Key Words : Low Dimensional Compounds; Ferromagnetic Compounds; Incommensurate Structures; Magnetic Interactions

INTRODUCTION

ONE of the most important and influential developments in solid state chemistry in the last ten years has been the identification and study of compounds in which the major interactions between the constituent ions or molecules take place in fewer than three dimensions. Thanks to the ingenuity of organic and inorganic chemists, compounds have been made with properties that challenge theory, like one-dimensional metals, or with combinations of properties not previously found in association with one another, like ferromagnetism and optical transparency or superconductivity in molecular crystals. Some of the special properties associated with low dimensionality are displayed in Table I. Of course, low-dimensional materials like micas or graphite have been known for many years and hundreds, if not thousands of solids contain layers or chains of closely spaced atoms or ions. However, the adjective 'low-dimensional' has come into use principally to describe physical properties that arise from the collective behaviour of electrons on lattices confined to one, or to two orthogonal axes. Two simple examples will illustrate the point.

In 1955, Peierls[1] pointed out that a one-dimensional electron gas is inherently unstable with respect to any lattice distortion with periodicity $1/2\ k_F$ equivalent to the wave-vector k_F at its Fermi Surface. This occurs because the energy of the occupied electron energy levels is lowered, and that of the

*Presented at the INSA Golden Jubilee Symposium on Solid State Chemistry held at INSA, New Delhi during December 4–6, 1985.

TABLE I

Some properties of low dimensional compounds

Property	Chain	Example	Layer
Structures			
Intercalation	$(SN)_x$—Br_2	TaS_2 + amines or organometallics $NiPS_3$ FeOCl	
Molecular composites		$(C_7H_{15}$ $CH_2NH_2)_2MNCl_4$ (gly-diac-gly) $CdCl_4$	
Phase transitions in organic groups	$((CH_3)_4N)MnCl_3$	$(CH_3NH_3)_2CdCl_4$	
Magnetism			
Low dimensional magnetism	$CsNiF_3$	Mn stearate	
Metmagnetism	Co (pyridine)$_2$ Cl_2	$FeCl_3$	
Transition to long range order	$AFeCl_3$ (A = K, Rb, Tl, Cs)	$(RNH_3)_2MCl_4$ (M = Cr, Cu)	
Conductivity			
Molecular metals	Ni (porphyrin) I	Graphite and BN salts	
Peierls instability	$K_2Pt(CN)_4Br_{0.30}3H_2O$	—	
Charge density wave	$NbSe_3$	NbS_2	
Superconductivity	$(SN)_x$ $Hg_{2.86}AsF_6$	TaS_2	

unoccupied ones raised, when the lattice periodicity is increased from a a/n_e, where n_e is the fractional band filling (or average number of valence electrons per atom in the tight-binding approximation). A gap in the energy spectrum then opens at k_F and the lattice undergoes a transformation from metallic to semi conducting. The Peierls theorem is only exact in one dimension because the requirement of a unique k_F value is only satisfied under those conditions. Consequently, a search began in the 1970's for one-dimensional metals. Coordination chemistry provides some of the clearest examples, the mixed valency Pt chain compounds such as KCP ($K_2Pt(CN)_4Br_{0.30}3H_2O$), and the predictions of Peierls were verified in detail.[2]

A second example is one-dimensional magnetism. It can be shown quite easily that a chain of localized moments interacting *via* near-neighbour ferro-or antiferromagnetic Ising exchange cannot exhibit infinite range order at any temperature above absolute zero, and hence, has no phase transition from an ordered to a disordered state. This is because the enthalpy required to reverse one spin in the otherwise completely ordered lattice is outweighed by the entropy gain arising from the fact that the spin reversal can take place at any site with equal probability. As I shall describe later in this article, the argument is

more subtle for other interaction Hamiltonians and higher dimensionality because, for example, 'domains' of reversed spins within three-dimensional lattice can have a wide veriety of shapes, and hence domain boundary energies. Surprisingly good approximations to one-dimensional ferro- and antiferromagnets exist, the most widely studied being those with structures related to the hexagonal perovskite lattice, e.g. $CsNiF_3$ and $N(CH_3)_4MnCl_3$. In the latter, the mean field transition temperature estimated from the measured near-neighbour exchange constant is 90 K while the Neel temperature is only 0.83 K. The optical spectra also reveal the dominant role of shor range order, even down to very low temeratures.[3]

To engineer interaction pathways confined to one or two dimensions alone, one frequently has to construct chemically quite elaborate structures, as Table I shows. Quite unusual opportunities for new kinds of physical behaviour then arise. For example, the role of molecular librational modes in the electron-phonon coupling responsible for the superconductivity of charge transfer salts is quite unknown. Low dimensionality also provides a structural mechanism for combining inorganic continuous lattices with organic molecular ones. Thus an inorganic layer may have organic molecules bond to it ionically, covalently or by metal-ligand coordination to make what we have called a 'molecular composite'.[4] The potential therefore exists to combine within the same crystal properties characteristic of the inorganic solid state, such as cooperative magnetism, and those more familiar from organic molecular solids like mesomorphism or topochemically steered solid state polymerization.

Both in the matter of finding paradigm examples of soluble physical models, and in synthesising new compounds with unlooked for properties, there has been intense world-wide activity for number of years. Reviews may be found in Miller (1982) and Gillespie and Day (1985).[5,6] In this brief article, it will not be possible to give more than a selective summary of that part of our own recent work on low-dimensional solids concerning magnetic interactions, to illustrate the richness of phenomena being uncovered.

Low-dimensional Ferromagnets

Ferromagnetic near neighbour exchange is quite rare in insulators, and usually is found only when the topology of the lattice forces a cancellation of competing antiferromagnetic exchange pathways. This is more likely to be the case in low-dimensional lattices because there is then a smaller number of equivalent 'bonds' between neighbours, and a smaller number of effective second and third near neighbours. There are two types of cation-anion-cation pathway which give rise to ferromagnetic exchange by the conventional super-exchange mechanism, and we have studied numerous examples of each.

Within a basic dimeric unit the requirement that unpaired spins on the two metal ions should align ferromagnetically is achieved if they occupy orthogonal orbitals. Given that metal-ligand covalency is not negligible, the necessary

orthogonality can be assured in principle in either of two ways.[7] The first requires that the cation orbitals containing the unpaired spins overlap orthogonal orbitals on the bridging ligand, and the second that spin density is delocalized from one cation through an intervening anion orbital to an unoccupied orbital on the other cation. The latter unoccupied orbital is necessarily orthogonal to the other orbitals of the *d*-subshell that contain the remaining unpaired electrons. For the case of *d*-orbitals overlapping ligand *p*-orbitals these two situations are shown in Fig. 1.

To engineer orthogonality between two *d*-orbitals of identical point symmetry on neigbouring lattice sites, of the kind shown in Fig. 1(*b*), the principal axes of the ligand fields around the two sites must themselves be orthogonal. This is realized most effectively through the mechanism of a cooperative Jahn-Teller distortion, the $3d^9$ and high spin $3d^4$ configurations being the ones most subject to such distortion. K_2CuF_4 was the first example of a crystal which become ferromagnetic by this mechanism (T_c 6.4K).[8] Based on the K_2NiF_4 structure, alternate corner-sharing octahedra are elongated along [100] and [010], ensuring that the half filled x^2-y^2 on one site is orthogonal to x^2-y^2 on each of its neighbours. Our own work has concerned the corresponding Cr(II) compounds A_2CrX_4, where A = Rb, Cs, RNH$_3$ and X = Cl, Br, I.[9] Here the problem is more complicated because the unpaired electron in the $e_g(O_h)$ subset occupies z^2 in an elongated D_{4h} site, and the three other electrons of the $3d^1$ configuration occupy xz, yz, xy. The z^2 orbital on site a (Fig. 2) overlaps with a $p\sigma$ orbital on the bridging halide ion, which in turn overlaps x^2-y^2 on site *b*.

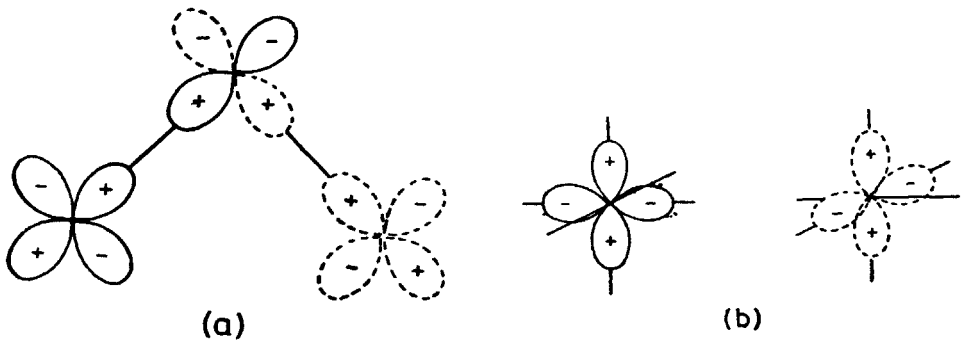

FIG 1 Two ways of achieving orthogonality between *d*-orbitals on adjacent metal ions. (*a*) Orthogonal orbitals on the bridging anion, (*b*) orthogonal *d*-orbitals.

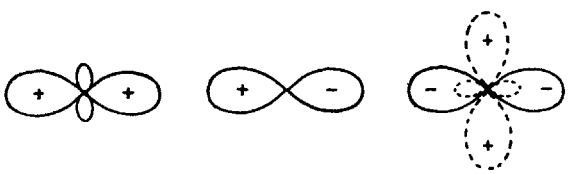

FIG 2 Superexchange pathway in A_3CrX_4 salts.

Repulsion between the four unpaired electrons on site *b* and the spin density in x^2-y^2 transferred from site *a* is minimized if they are all parallel, hence the exchange constant J_{ab} is again positive.

To test this orbital ordering model we have performed single crystal polarised neutron diffraction measurements on Rb_2CrCl_4 at 4.5 K.[10] Magnetic structure factors F_M were derived from the flipping ratios of 660 main structure reflections, whose intensity is derived mainly from the Cr^{2+} and Rb^+ sites and 57 'superlattice' reflections, whose intensity derives from the displacement of the basal plane Cl^- ions by the cooperative Jahn-Teller distortion. The F_M were modelled by representing the magnetization density as a superposition of densities from 3*d* and 4*s*-orbitals on Cr^{2+} and 3*s* and 3*p* centred on Cl^-. As well as allowing the total 3*d* and 4*s* moments on Cr^{2+} to vary in the least squares refinement, the proportion of the the 3*d* moment residing in each of five orbitals was also refined with the following result : *yz* 0.26(2), *xz* 0.25(2), *xy* 0.25, z^2 0.25(2) and x^2-y^2 −0.01(2). Thus the orbital ordering model is completely vindicated. In addition to the moment localized on the Cr^{2+} ($3.16\mu_B$ in 3*d* and $0.6\mu_B$ in 4*s*) a small spin transfer to the Cl^- was also detected, amounting to $0.06\mu_B$ on on those lying in the basal plane and $0.08\mu_B$ on those in the axial sites.

The ground state in the A_2CrX_4 compounds has $S = 2$, instead of $S = O$ for K_2CuF_4, and *J* is somewhat larger because of increased metal-ligand covalency, which arises partly from the heavier halogen and partly from the larger radial extension of the 3*d*-orbitals nearer the beginning of the *d*-block. Consequently T_c is increased to the region of 50 K. Wide chemical variation is possible within the A_2CrX_4 series, and representative values of *J* and T_c are shown in Table II. One of the most significant variations is in the interlayer separation, tuned by the organic sidechain *R* in RNH_3^+, and these are also listed in Table II. Below, we shall discuss the nature of the phase transition in these two-dimensional lattices.

TABLE II

Exchange parameters, Curie temperatures and inter-layer spacings in two-dimensional ferromagnetic tetrachlorochromate (II) salts

	J/*K*	T_c/*K*	Interlayer spacing
Rb_2CrCl_4	14.4	52.4	7.88
Rb_2CrCl_3Br	—	55.0	8.03
$Rb_2CrCl_2Br_2$	—	57.0	8.19
$Rb_2CrCl_2I_2$	—	61	8.68
$(CH_3NH_3)_2CrCl_4$	13.0	42.0	9.44
$(CH_3CH_2NH_3)_2CrCl_4$	10.1	41.0	10.71
$(CH_3(CH_2)_2NH_3)_2CrCl_4$	9.3	39.5	12.35
$(C_6H_5CH_2NH_3)_2CrCl_4$	10.6	37.0	15.71
$(CH_3(CH_2)_4NH_3)CrCl_4$	9.3	—	17.81
$(H_3N(CH_2)_3NH_3)_2CrCl_4$	10.6	—	—
$(CH_3(CH_2)_{11}NH_3)_2CrCl_4$	9.6	—	31.0

The second mechanism for achieving near-neighbour ferromagnetic exchange in Fig. 1 requires a cation-anion-cation bridging angle in the region of 90°. The best approximations to such a situation in low-dimensional continuous lattice compounds are found in two major classes of compound, the one-dimensional hexagonal perovskites ABX_3 and the layer salts with $CdCl_2$ or CdI_2 structures. In all the halides MX_2 (M = Fe, Co, Ni; X = Cl, Br, I) J is ferromagnetic, though the much weaker interlayer exchange J' is antiferromagnetic, so the three-dimensional magnetic structure is of the metamagnetic type. The octahedral BX_6 unit in ABX_3 share opposite faces, so the B-B distance is quite small and direct exchange, rather than superexchage is sometimes more important. Neveitheless, positive J is found in compounds with B = Fe and Ni though the sensitivity of the ordering mechanism may be judged from Table III, which indicates the sign of J in ABX_3 (B = Fe, Ni) as a function of A and X.

TABLE III

Sign of the nearest neighbour exchange constant in hexagonal perovskites ABX_3 (B = Fe, Ni)

	Fe			*Ni*	
X = Cl	Br	F	Cl	Br	
A = K +	—	.	—	.	
Rb +	—	.	—	—	
Cs +	—	+	—	—	
$N(CH_3)_4$.	.	.	+	+	

Competition between direct exchange, and competing 90° and 180° B-X-B superexchange in these compounds is demonstrated quite neatly by examining the effect of hydrostatic pressure on the magnetic order. Thus in $RbFeCl_3$ with a Fe-Cl-Fe angle of 74.6° J is ferromagnetic while in $RbFeBr_3$, where it is 72.4° J is antiferromagnetic. Applying a hydrostatic pressure of 5Kbar to the former reduces the Fe-Cl-Fe angle below the corresponding angle in the bromide, yet J remains ferromagnetic and T_N increases from 2.5 to 6.5 K because anti-ferromagnetic interchain coupling increases.[14]

COMPETING INTERACTIONS: CANTED AND INCOMMENSURATE STRUCTURES

Nature rarely provides compounds in which a near-neighbour ferromagnetic exchange is the only interaction bringing about long range order. In practice, single ion anisotropy, dipolar interaction between chains or layers ordered spins, and exchange between more remote ions may all contribute to complicate the situation and introduce unusual types or order. In this section, a few examples from the work of our group on low-dimensional ferromagnets will be summarized.

As already noted, the single ion ground state in the A_2CrX_4 ferromagnet is a quintet (^5A_g in the D_{2h} crystal field). Therefore, in contrast to K_2CuF_4, single ion anisotropy must be included in the hamiltonian. The principle axes of the g-tensors

on neighbouring sites are orthogonal because of the cooperative Jahn-Teller distortion and so also are the planar anisotropy terms. In the absence of exchange alternate Cr^{2+} moments would be directed along [100] and [010] of the parent K_2NiF_4-type cell. The ferromagnetic near-neighbour exchange rotates the moments towards the easy [110] direction but competition with the single ion anisotropy ensures that the moments retain a small ($\sim 3°$) canting alternately to one side and the other of this axis (Fig. 3). The canting reveals itself by the presence of very weak purely magnetic reflections in the neutron diffraction,[10] and by a small anisotropy gap in the spin-wave density-of-states at the centre of the Brillouin zone, which has important consequences for the behaviour of the optical absorption spectrum at very low temperatures. It also affects the critical behaviour, described later.

Another form of competition between ferromagnetic exchange and single ion anisotropy occurs in the one-dimensional hexagonal perovskites $A FeCl_3$ (A = Rb, Cr) where the dominant octahedral component of the crystal field gives a single ion ground state $^5T_{2g}$. First-order spin-orbit coupling lifts the degeneracy to leave a $J = 1$ level lying lowest, and this is further split by a more minor trigonal crystal field component into $M_J = 0$ and ± 1. In contrast to the situation in the two-dimensional $FeCl_2$, the singlet lies lower in energy than the doublet. Hence in the absence of an exchange field, or an externally applied field, the ground state is non-magnetic. The exchange field due to the near-neighbour ferromagnetic coupling induces mixing between the $M_J = 0$ and ± 1 levels which, if large enough, can

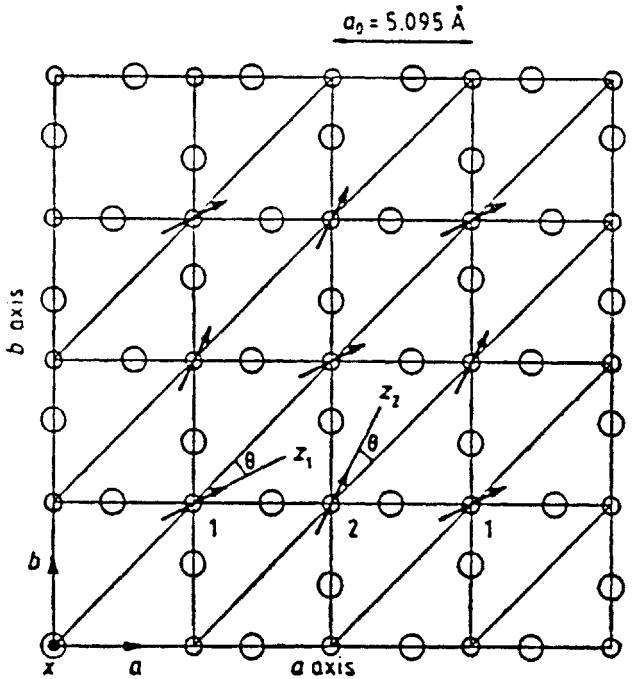

FIG 3 The canted spin structure of Rb_2CrCl_4.

lead to a long-range-ordered magnetic ground state. As noted above, J depends on the Fe–Cl–Fe angle, which also determines the singlet-doublet separation. The nature of the long range order is therefore extraordinarily sensitive to small changes in the structure. For example $RbFeCl_3$ undergoes a transition to three-dimensional order, with easy-plane ferromagnetic chains, at 2.55K while $CsFeCl_3$ has no such transition down to 80mK. On the other hand order can be induced in the Cs compound by an applied field. Thus the magnetic phase diagrams of these two compounds are quite different, as shown diagramatically in Fig. 4.

In a compound containing chains of ferromagnetically ordered spins like $RbFeCl_3$, the ordering between chains is determined by yet another kind of competition. Weak antiferromagnetic coupling alone between chains would lead to a 120° (triangular) arrangement of spins in the plane perpendicular to the chains, signalled by magnetic neutron scattering intensity at (1/3, 1/3, 0) with respect to the 'chemical' unit cell. However, since the chains are ferromagnetic, they act as giant dipoles, between which the free energy is minimized if the dipoles are collinear. Consequently, on passing $T_N = 2.55$K, neutron scattering intensity appears first at $(1/3 + \delta, 1/3 - \delta, 0)$ with $\delta \sim 0.018$, then moves to $(1/3 - \delta', 1/3 - \delta', 0)$, $(\delta' = 0.005)$ at 2.35K and finally to (1/3, 1/3, 0) at 1.9K.[13] An example of the scattered intensity distribution in the a*b* plane is given in Fig. 5(*a*).[14] For a $RbFeCl_3$ crystal doped with 5 per cent Cs^+ and the quite comparable evolution of the incommensurate ordering in $CsFeCl_3$ as a function of applied field in Fig. 5(*b*).[15]

Finally, a more classical source of incommensurate magnetic ordering is the competition between first, and more remote, neighbour exchange constants of opposed sign. For a two-dimensional triangular lattice Rastelli *et al.*[16] calculated the relative stabilities of different spin structures as a function of $j_n = J_n/J_1$, with the result shown in Fig. 6. Clearly, when J_1, J_2 and J_3 (defined for the $CdCl_2$ lattice in Fig. 7) are all positive, as in the top right hand quadrant of Fig. 6, the order is simply ferro-magnetic (phase I). This is the situation in CoX_2 (X = Cl, Br, I)

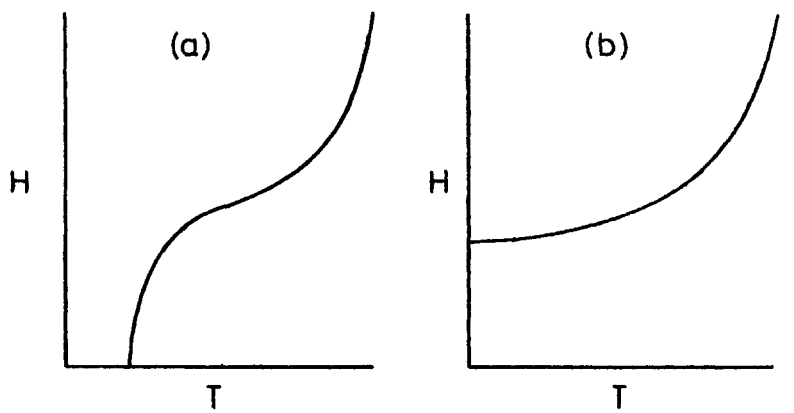

FIG 4 Magnetic phase diagrams in the H, T plane for (*a*) $RbFeCl_3$ (*b*) $CsFeCl_3$.

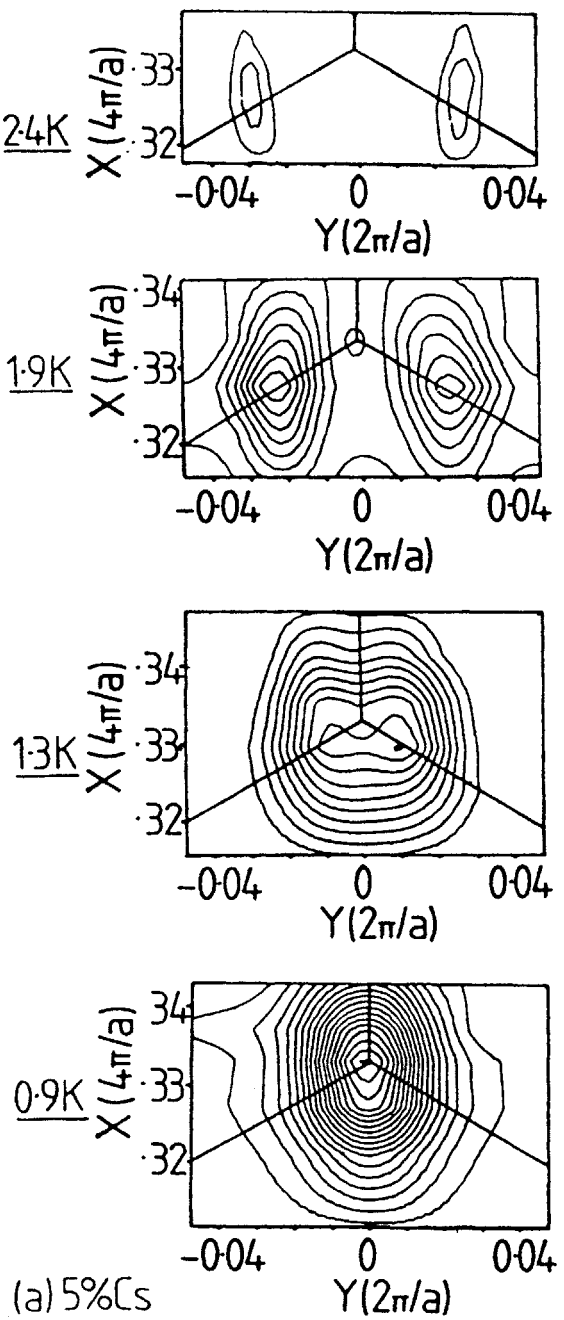

FIG 5 Incommensurate magnetic structures of $A FeCl_3$ (*a*) Neutron scattering profile around (1/3, 1/3, 0) in $RbFeCl_3$ at 2.2K.[14]

and $NiCl_2$. However, exceptionally in $NiBr_2$ $j_3 = -0.28$ and $j_2 \sim 0$, placing it within the stability range of a helical phase with propagation vector τ along [110]

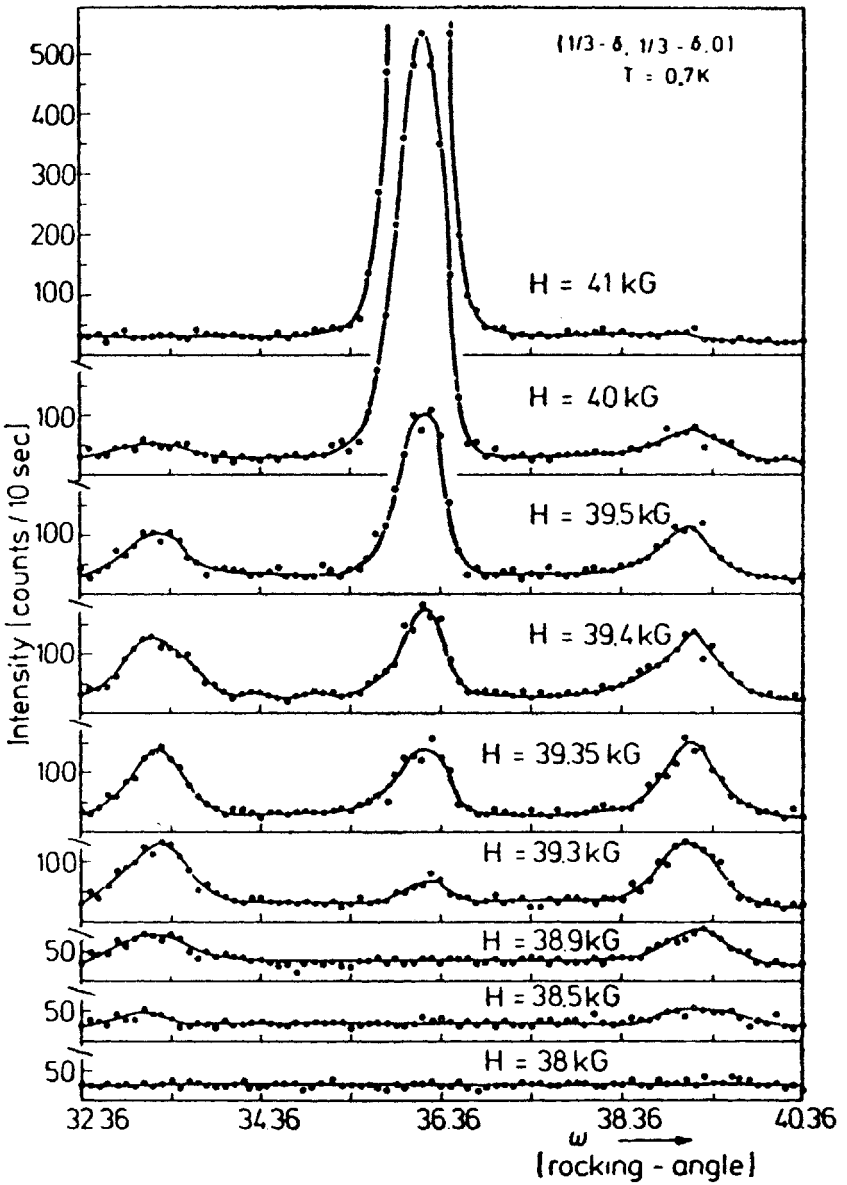

FIG 5 (*b*) Evolution of neutron scattering intensity at (1/3-δ, 1/3-δ, 0) in $CsFeCl_3$ as a function of field.[15]

(phase IV, Fig. 6) very close to the boundary with phase I. Single crystal neutron diffraction at 4K, using a multidetector to sample a region of reciprocal space around the (0, 0, 3/2) reciprocal lattice point, reveals the resulting incommensurate structure with $\tau = 0.027$ (Fig. 8(*a*)).[17] Remarkably, substituting $NiBr_2$ with 9 mole per cent Fe^{2+} causes τ to move to [100] (phase III) (Fig. 8(*b*)).[18]

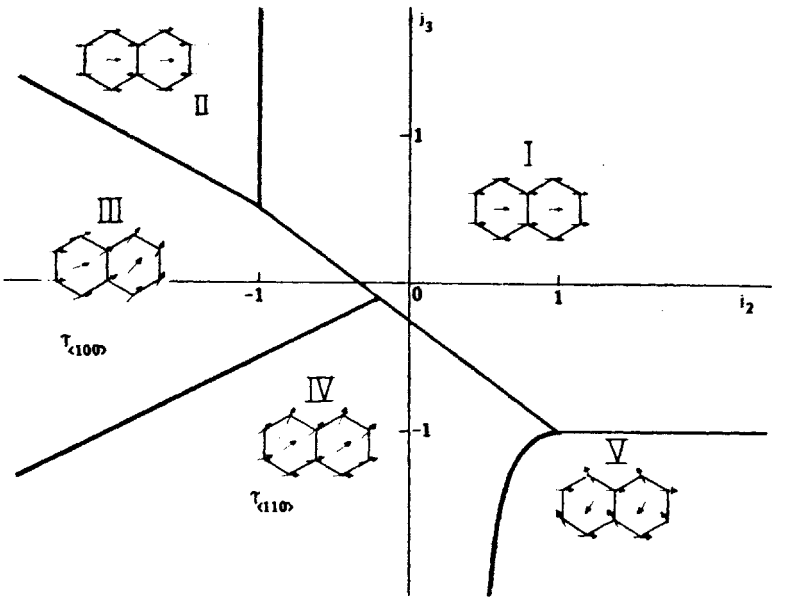

FIG 6 Magnetic phase diagram of a hexagonal planar lattice in the (j_2, j_3) plane,[16] where $j_n = J_n/J_1$.

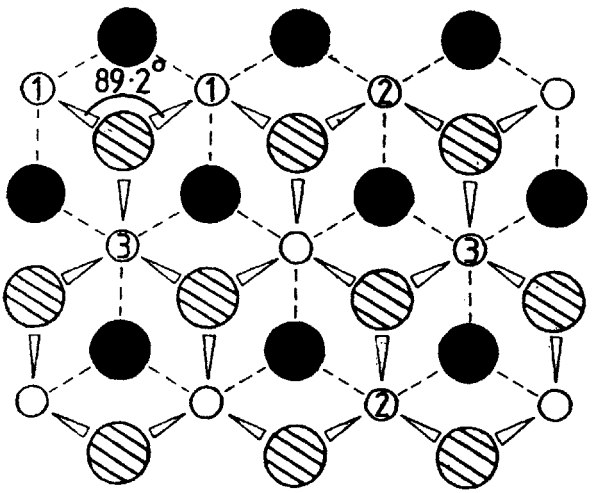

FIG 7 Intraplanar exchange constants J_n between (n, n) pairs in $NiBr_2$.

An even more remarkable feature of $NiBr_2$ is that the propagation length, measuring the 'pitch' of the helix, increases continuously with increasing temperature until at 23K it has become infinite[19] i.e. the moments are collinear as in Phase I. The collinear phase then remains stable up to T_N = 44K. Again, single crystal neutron diffraction provides the evidence for the phenomenon : Fig. 9 shows the

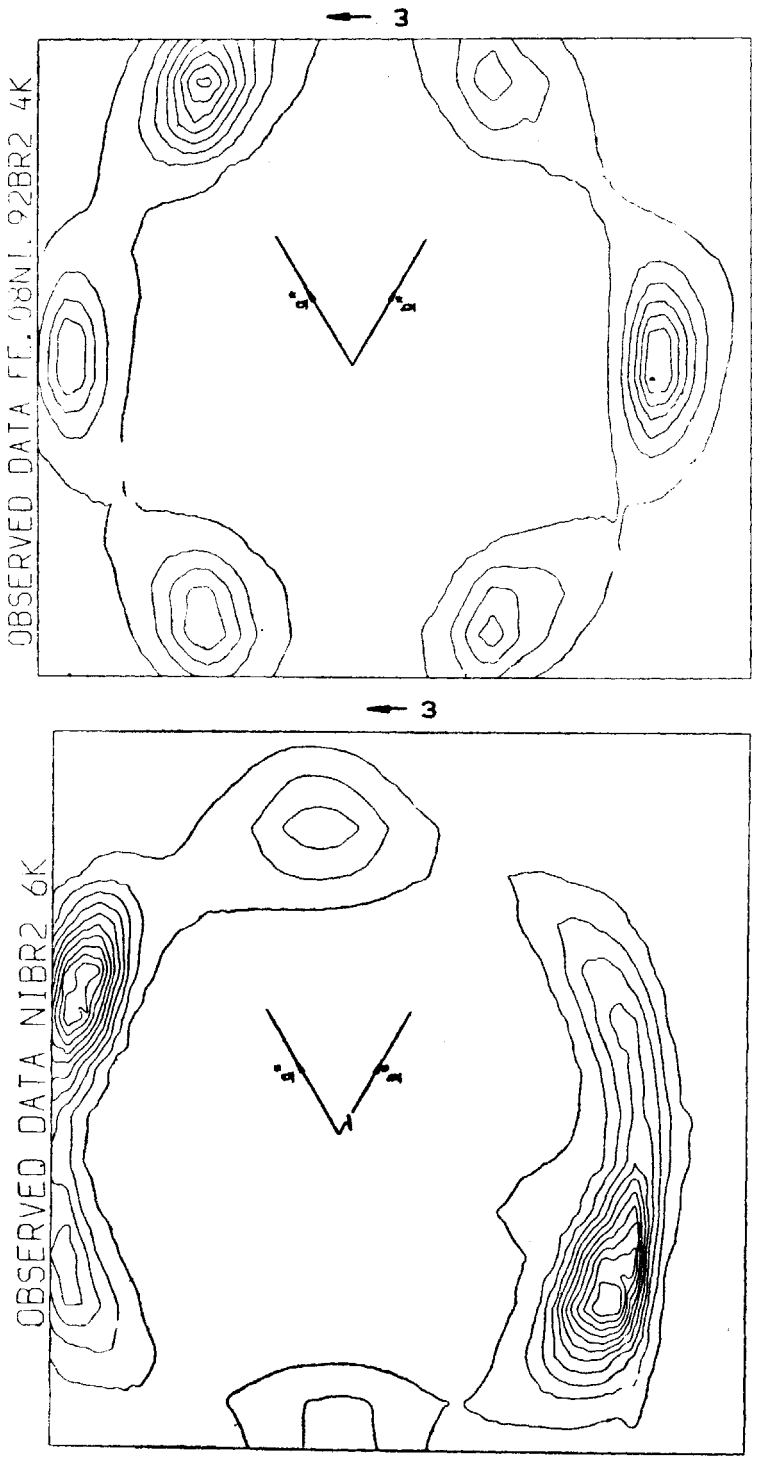

FIG 8 Neutron scattering intensity in the a^*b^* plane around (0, 0, 3/2) at 4.2K in (*a*) $NiBr_2$ (*b*) $Ni_{0.99}Fe_{0.01}Br_2$.

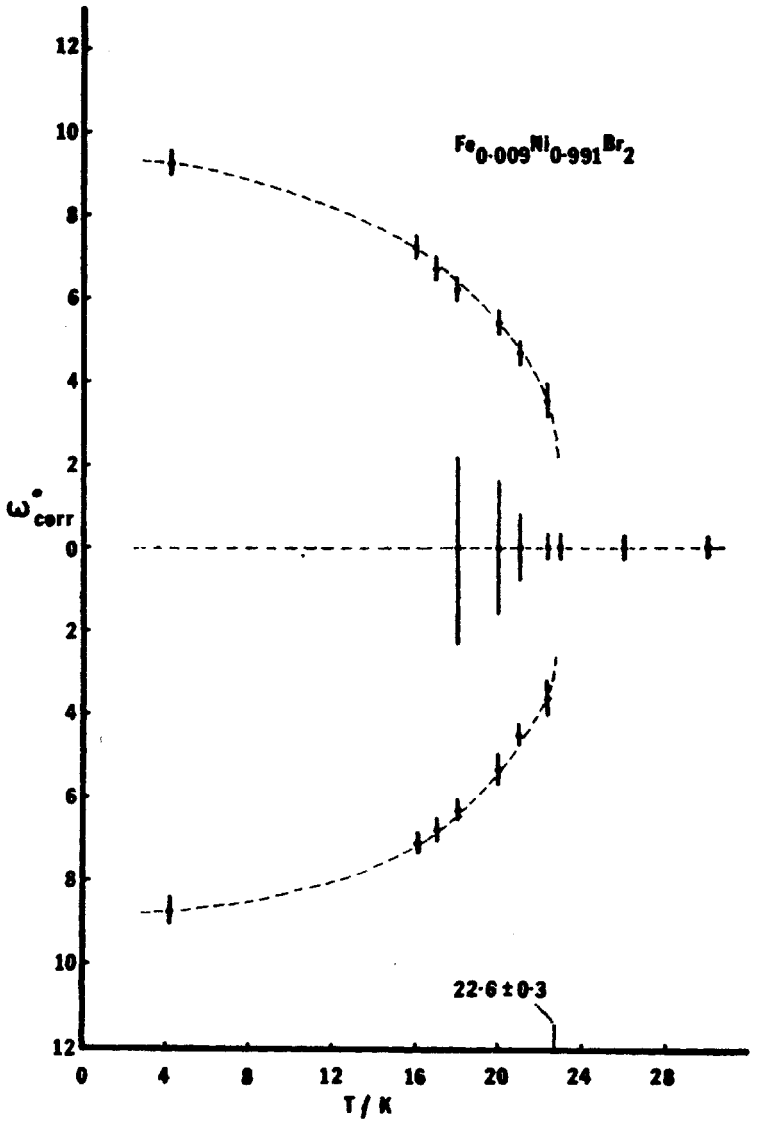

FIG 9 Temperature-dependence of the incommensurate propagation vector τ τ in $Ni_{0.99}Fe_{0.01}Br_2$.[18]

temperature dependence of τ, in a $NiBr_2$ crystal containing 1 mole per cent Fe^{2+}, in which τ still lies along [110]. So far as is known, such behaviour is unique among magnetic insulators with localized moments, and at once raises the question 'what is its mechanism?' Lattice expansion would be a possible explanation since the j_n ratios might be modified sufficiently for the system to cross the boundary from phase IV to phase I. However, this can be ruled out by performing neutron diffraction measurements under hydrostatic pressure.[20] With increasing pressure τ decreases, so the decrease in τ with increasing temperature cannot be due to an

increase in the lattice parameters. We have also measured the dispersion of the spin waves in $NiBr_2$ along [110], [100] and [001] by inelastic neutron scattering at 4K, when the magnetic structure is helical, and 30K when it is collinear.[21] No significant variation is found in any of the intralayer exchange constants, though there is a small decrease in the anisotropy constant and the interlayer exchange constant. A theoretical explanation of this very unusual phenomenon has recently been given by Rastelli and Tassi[22] in terms of magnon-magnon interactions.

The Transition to Long Range Order

A fundamental question in any low-dimensional magnetic system concerns the mechanism of the transition to the long range ordered state. As mentioned in the Introduction, a one-dimensional array of Ising spins is predicted to have no long range order above 0 K and the same is true of a two-dimensional Heisenberg ferromagnet. On the other hand the two-dimensional Ising ferromagnet was shown to be capable of having a phase transition at finite temperature by Onsager.[23] In contrast the two-dimensional XY model (i.e. of spins constrained within a plane) was only teckled theoretically much more recently. Kosterlitz and Thouless[24] (KT) showed that a phase transition in such a structure could occur at a temperature T_{TK} by the binding of pairs of vortices of spins with opposite chirality. A vortex is a system of spins constrained to rotate in the plane of the lattice. An example of a Monte Carlo simulation of the equilibrium spin configuration in an XY ferromagnet at $0.5T_c$ is given in Fig. 10,[25] where the vortices of rotated spins are enclosed by the broken lines. For any temperature below T_{KT} the KT theory requires that

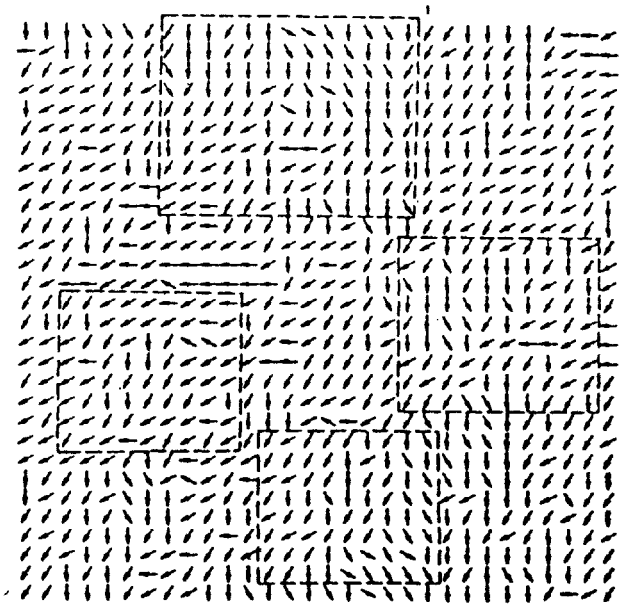

Fig 10 Monte Carlo simulation of spins in a two-dimensional XY lattice at $T = 0.5T_c$.[25]

the susceptibility χ remains infinite. Therefore, all temperatures less than T_{KT} are critical are critical points and the magnetization should obey the relation.

$$\lim_{H\to 0} \langle M \rangle \propto H^{1/\delta(T)} \qquad \ldots(1)$$

Although they retain a very small anisotropy within the basal plane the A_2CrX_4 compounds are expected to be quite good approximations to two-dimensional XY ferromagnets. Fig. 11 shows the magnetization of a single crystal of Rb_2CrCl_4 *vs* field along the easy [110] direction at temperatures between 6.6 and 79K, measured by Faraday magnetometry.[26] It can be seen that eq. (1) is indeed obeyed up to 47K. The variation of the exponent $\delta(T)$ with temperature is also in accordance with the prediction of the KT theory.

The experimental signature of KT theory at temperatures above T_{KT} is a divergence of χ according to the formula

$$\chi(T) = A \exp(B^* t^{-1/2}), \qquad \ldots(2)$$

where $t = (T - T_{KT})/T_{KT}$. This should be contrasted with the conventional power law theory of critical exponents,[27] from which one would predict

$$\chi^T = C(t_+)^{-\gamma}, \qquad \ldots(3)$$

where $t = (T - T_c)/T_c$. For Rb_2CrCl_4 we find that the high temperature susceptibility fits eq. (2) very well (goodness of fit parameter $\chi^2_G = 9.6$) though nearly as good a fit can be obtained with eq. (3) ($\chi^2_G = 13.1$). Further verification of the KT

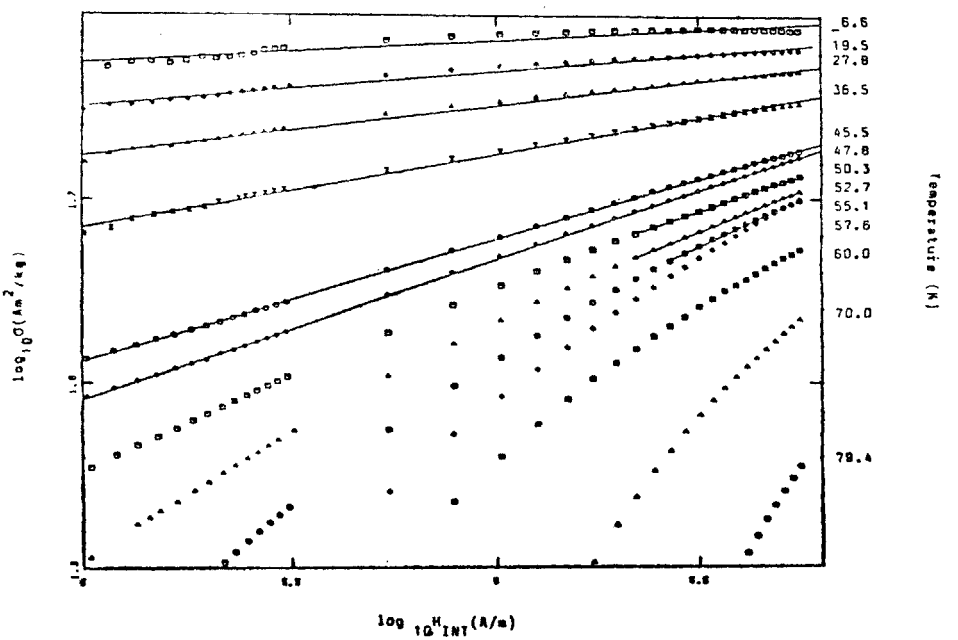

FIG 11 Magnetization isotherms of Rb_2CrCl_4 from 6 to 80 K.[26]

theory for Rb_2CrCl_4 is being sought by neutron scattering in the critical region. Monte Carlo simulations of the scattering function $S(Q, \omega)$ for a two-dimentional XY ferromagnet suggest that the energies of the longest wavelength spin-waves should drop sharply to zero at T_c and that a central component should appear in the scattering. Both features are indeed observed[28] but more quantitative analysis is needed before we can be sure of their source.

Chemical variation within the A_2CrX_4 series makes it possible to examine how the critical properties are affected by changes in the inter-layer interactions. These may be brought about in two ways : either one can simply change the inter-layer separation, as in the $(RNH_3)_2CrCl_4$ series whose magnetic parameters are listed in Table II, or one can change the axial halide ions and hence modify the inter-layer exchange constant.[29]

Already in Rb_2CrCl_4 the ratio of intra- to inter-layer exchange constants is 10^3 so increasing the inter-layer separation further must render the RNH_3^+ salts even better approximations to pure two-dimensional systems. The T_c's fall as inter-layer spacing increases, but this is due in part to a drop in J. The latter is due in turn to a small puckering of the Cr–Cl layers as a result of the need to accommodate the organic sidechains and the weak hydrogen-bonds formed between the NH_3^+ and the axial and equatorial Cl^-. For example, puckering decreases the Cr–Cl–Cr angle from 180° in Rb_2CrCl_4 to 160° in $(CH_3NH_3)_2CrCl_4$.[30] In Fig. 12, the measured

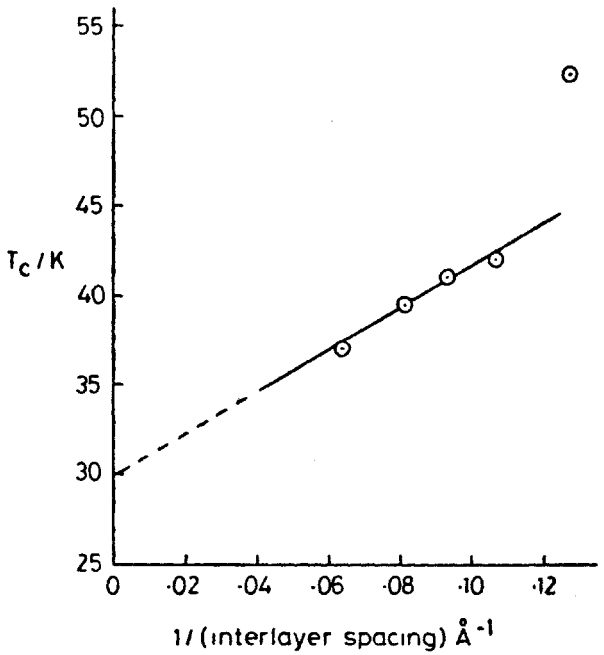

FIG 12 Curie temperatures of A_2CrCl_4 *versus* inverse interlayer separation.

T_c are plotted against the reciprocal of the interlayer separation, so that an extra polation can be made to infinite separation. T_c tends to a finite value in the region of 30K, which represents the transition temperature $T_c(2)$ of a purely two-dimensional tetrachlorochromate(II) ferromagnet. It is instructive to compare this estimate with the value predicted by the formula given by Stanley and Kaplan. These authors found that for $S \geqslant \frac{1}{2}$ a transition could occur in a two-dimensional Heisenberg or XY system at a finite temperature $T_c(2)$ to a state in which χ diverged but in which there was no long range order. If a small Ising-like anisotropy existed a transition to a long range ordered state would take place at a temperature $T_c \sim T_c(2)$. For a number of nearest neighbours $z = 4$ and $S = 2$ the Stanley-Kaplan formula

$$T_c(2) \sim \left(\frac{1}{10}\right)(z-1)\,[2S(S+1)-1]\,\frac{J}{K} \qquad \ldots(4)$$

predicts $T_c(2) \sim 35$K if we take the average of the J in Table II.

As a low-dimensional magnetic system approaches the transition to a three-dimensionally ordered state from below, one anticipates a change in the spatial (d) and spin (n) dimensionality as follows:

$$d \leqslant 3 \rightarrow d = 3$$
$$n = 3 \rightarrow n \leqslant 3$$

These changes should manifest themselves in a 'crossover' in the critical exponent β of the magnetization with increasing temperatures. To measure the zero-field (spontaneous) magnetization we use the intensity of magnetic elastic neutron scattering. Taking the tetrahalogenochromates as example in Rb_2CrCl_4 β changes from 0.23 to 0.33 at 0.8K below T_c,[31] while in $Rb_2CrCl_2Br_2$ a similar change takes place from 0.26 to 0.41 about 3K below T_c.[32] The Br^- in the latter salt occupy the axial sites in the K_2NiF_4-like structure[33] so one expects the inter-layer exchange to be stronger than in Rb_2CrCl_4. Predicted values of β for three-dimensional Ising and Heisenberg models are 0.31 and 0.38 respectively. The values of 0.23–0.26 further below T_c are comparable to those found in other two-dimensional XY systems such as $CoBr_26H_2O$ ($\beta = 0.26$)[34] and K_2CuF_4 ($\beta = 0.22$).

Conclusion

This account has concentrated on some recent examples from low-dimensional magnetism to show some of the richness and subtlety of physical phenomena that arise when interactions are confined to layers or chains within a lattice. Synthetic chemistry has brought to light many beautiful new systems, for example the transparent ferromagnets and temperature dependent helices. It has also made possible the systematic variation of parameters so that the limits of the abstract theoretical models can be probed. More surprises are undoubtedly in store, for the real world of chemistry is always more complicated than the model of theoretical physics.

ACKNOWLEDGEMENT

My thanks are due to the Indian National Science Academy for the opportunity to present this survey.

REFERENCES

1. R Peierls *Quantum Theory of Solids* Clarendon Press Oxford (1955)
2. J M Williams A J Schultz A E Underhill and K Carneiro In : *Extended Linear Chain Compounds* (*Ed* J S Miller) Plenum Press New York (1982)
3. P Day and L Dubicki *J chem Soc Farady Trans* II **69** (1973) 363
4. P Day *Phil Trans R Soc* **A314** (1985) 145
5. J S Miller (*Ed*) *Extended Linear Chain Compounds* Plenum Press New York (1985)
6. R Gillespie and P Day *Electrical and Magnetic Properties of Low-Dimensional Solids* Royal Society London (1985)
7. J B Goodenough *Magnetism and the Chemical Bond* Interscience New York (1963)
8. H Ikeda and K Hirakawa *J phys Soc Japan* **33** (1972) 393
9. P Day *Accts chem Res* **12** (1979) 236
10. P Day P J Fyne E Hellner M T Hutchings G Munninghoff and F Tasset *Proc R Soc London* (1985) *In Press*
11. E Janke M T Hutchings P Day and P J Walker *J Phys C : Solid State Phys* **16** (1983) 5959
12. E Janke T E Wood C Ironside and P Day *J Phys C : Solid State Phys* **15** (1982) 3809
13. H Shiba and N Suzuki *J phys Soc Japan* **51** (1982) 3488
14. A Harrison D Visser P Day W Knop and M Steiner (1985) *To be published*
15. W Knop M Steiner and P Day *J Magn Mat* **31–34** (1983) 1033
16. E Rastelli A Tassi and L Reatto *Physica B* (*Amsterdam*) **97** (1979) 1
17. P Day M W Moore C Wilkinson and K R A Ziebeck *J Magn Mater* **50** (1985) 1
18. M W Moore and P Day *J Solid State Chem* **59** (1985) 23
19. P Day and K R A Ziebeck *J Phys C : Solid State Phys* **13** (1980) L523
20. P Day and C Vettier *J Phys C : Solid Stat Phys* **14** (1981) L195
21. P Day M W Moore T E Wood D Mc K Paul K R A Ziebeck L P Regnault and Rossat-Mignod *Solid State Commun* **51** (1984) 627
22. E Rastelli and A Tassi *J Magn Mater* **S4–S7** (1986) in press
23. L Onsager *Phys Rev* **65** (1944) 117
24. J M Kosterlitz and D J Thouless *J Phys C : Solid State Phys* **6** (1973) 1181
25. S Miyashita H Nishimori A Kuroda and M Suzuki *Progr Theor Phys* **60** (1978) 1669
26. C A Cornelius P Day P J Fyne M T Hutching and P J Walker *J Phys C : Solid State Phys* (1985) *in press*
27. H E Stanley *Introduction to Phase Transition and Critical Phenomena* Oxford University Press Oxford (1971)
28. M T Hutching P Day E Janke and R Pynn *J Magn Magn Mater* **S4–S7** *in press*
29. P Day *J Magn Magn Mater* **S4–S7** *in press*
30. C Bellitto T E Wood and P Day *Inorg Chem* **24** (1985) 558
31. J Als-Nielsen and M T Hutchings *Personal Communication* (1983)
32. S T Bramwell P Day M T Hutchings J R G Thorne and D Visser *Inorg Chem* (1985) *in press*
33. P J Fyne M T Hutching and P Day *Mater Res Bull* **20** (1985) 197
34. J A J Basten and A L M Bougaarts *Physica B + C* (*Amsterdam*) **86–88** *in press*